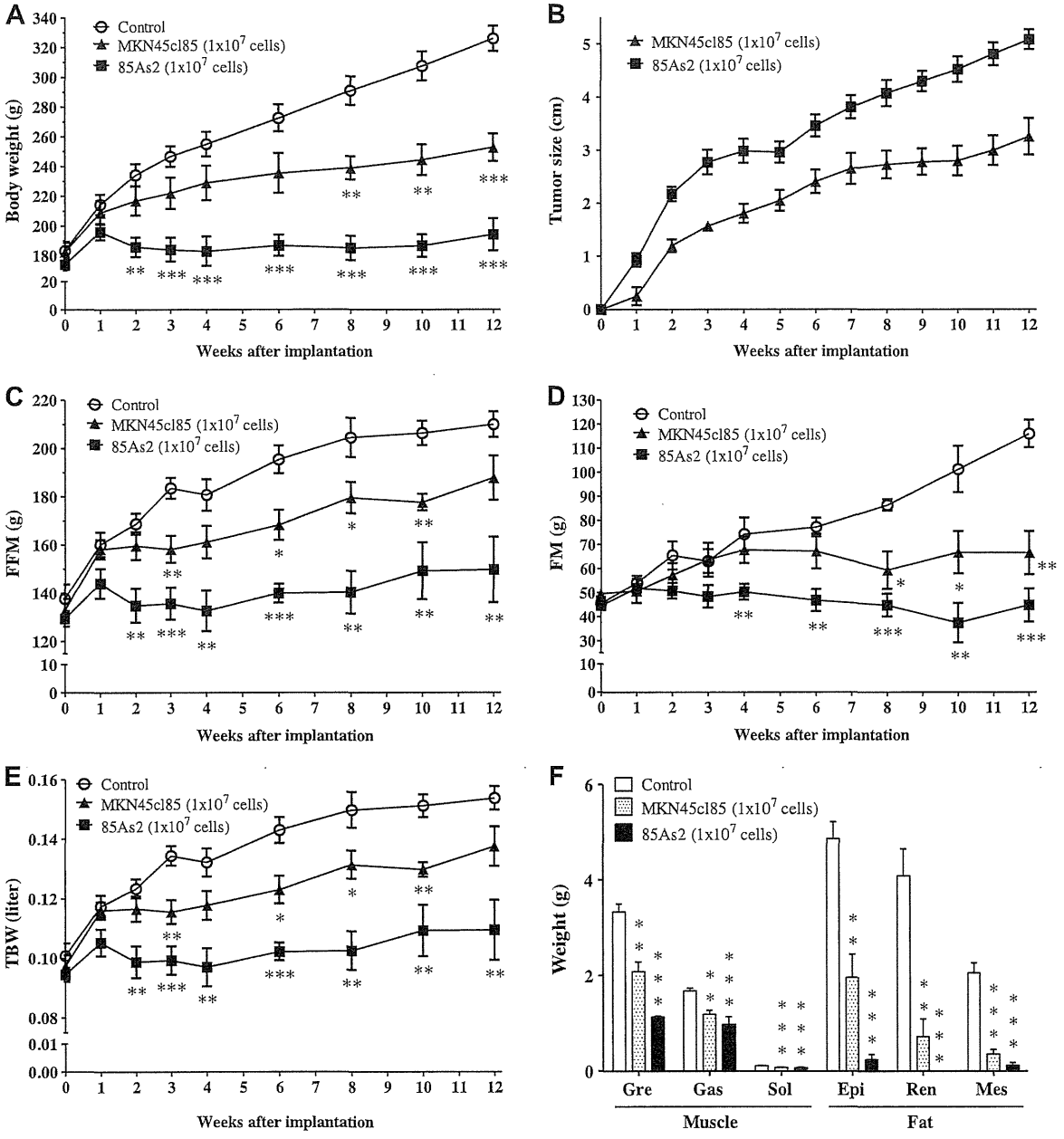

Fig. 1. Effects of MKN45cl85 and 85As2 cell implantation on body weight (*A*), tumor size (*B*), fat-free mass (FFM; *C*), fat mass (FM; *D*), total body water (TBW; *E*), and muscle and adipose tissue weights in nude rats (*F*). Rats were inoculated subcutaneously (sc) with MKN45cl85 or 85As2 cells in both flanks (1×10^7 cells/each site) at *week 0*. Rats inoculated with saline served as a control group. Each data point or bar represents the mean ± SE of 4–5 rats. Differences between groups were evaluated using Student's *t*-test or Welch's *t*-test. $^*P < 0.05$, $^{**}P < 0.01$, $^{***}P < 0.001$ vs. the control group. Gre, greater pectoral muscle; Gas, gastrocnemius muscle; Sol, soleus muscle; Epi, epididymal fat; Ren, perirenal fat; Mes, mesentery fat.

Cycler 480 software to analyze the exponential phase of amplification and the melting curve as recommended by the manufacturer. The amount of target mRNA in the experimental group relative to that in the control group was determined from the resulting fluorescence and threshold values (C_T) using the $2^{-\Delta\Delta C_T}$ method (37).

Cytokine measurements. Plasma levels of human IL-1β, IL-6, IL-8, TNFα, and LIF were measured using the Luminex Multiplex Assay (Affymetrix, Billerica, MA) (18). Rat IL-1β, IL-6, TNFα, keratinocyte-derived chemokine (KC), and interferon (IFN)γ plasma levels were measured using the Procarta Cytokine Assay Kit (Affymetrix). Plasma α1-acid glycoprotein and albumin levels were measured using a rat α1-acid glycoprotein enzyme-linked immunosorbent assay (ELISA) kit (Immunology Consultants Laboratory, Newberg, OR) and a rat albumin ELISA kit (Shibayagi, Gunma, Japan), respectively. Human cytokine levels were also measured in MKN45cl85 and 85As2 cell culture supernatants (5×10^5 cells/well) at 24 and 48 h.

In situ hybridization. In situ hybridization was performed as described previously (55). Briefly, frozen 12-μm-thick coronal brain sections were prepared in a cryostat at −20°C, thawed, and mounted onto gelatin/chrome alum-coated slides. The paraventricular nucleus

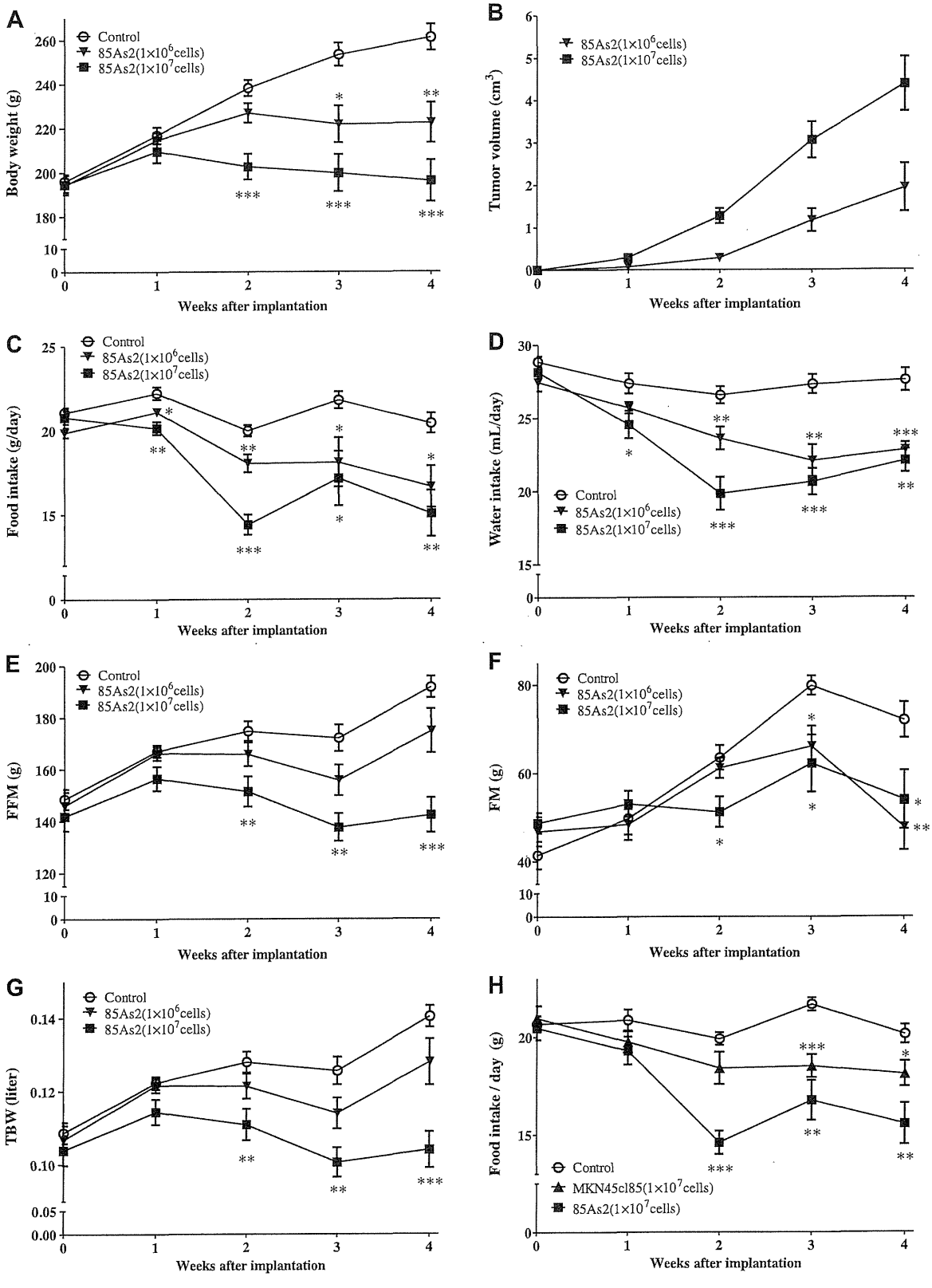
A
Body weight (g)
Control
85As2(1×10^6cells)
85As2(1×10^7cells)
Weeks after implantation
B
Tumor volume (cm^3)
85As2(1×10^6cells)
85As2(1×10^7cells)
Weeks after implantation
C
Food intake (g/day)
Control
85As2(1×10^6cells)
85As2(1×10^7cells)
Weeks after implantation
D
Water intake (mL/day)
Control
85As2(1×10^6cells)
85As2(1×10^7cells)
Weeks after implantation
E
FFM (g)
Control
85As2(1×10^6cells)
85As2(1×10^7cells)
Weeks after implantation
F
FM (g)
Control
85As2(1×10^6cells)
85As2(1×10^7cells)
Weeks after implantation
G
TBW (liter)
Control
85As2(1×10^6cells)
85As2(1×10^7cells)
Weeks after implantation
H
Food intake / day (g)
Control
MKN45cl85(1×10^7cells)
85As2(1×10^7cells)
Weeks after implantation

Table 1. *Body, tumor, muscle, fat, and organ weights in nude rats 4 wk after implantation with different 85As2 cell concentrations*

		85As2 Cells	
	Control	1×10^6	1×10^7
TW	0.00 ± 0.00	5.19 ± 1.54*	11.00 ± 2.31***,#
TV	0.00 ± 0.00	3.77 ± 1.27**	8.75 ± 1.50***,##
BW	259.62 ± 5.84	219.78 ± 8.98**	192.96 ± 8.62***
%control	100.0 ± 2.3	84.7 ± 3.5***	74.3 ± 3.3***
BW − CTW	259.62 ± 5.84	216.01 ± 10.18**	184.20 ± 9.25***,#
%control	100.0 ± 2.3	83.2 ± 3.9***	71.0 ± 3.6***,#
BW − TW	259.62 ± 5.84	214.59 ± 10.39***	181.96 ± 9.91***
%control	100.0 ± 2.3	82.7 ± 4.0***	70.1 ± 3.8***
Peak BW		226.89 ± 6.06	206.63 ± 7.15
%peak BW		94.4 ± 2.7	88.0 ± 3.5†
Muscle weights			
Greater pectoral	2.67 ± 0.11	1.88 ± 0.10***	1.42 ± 0.04***,##
Gastrocnemius	1.37 ± 0.04	1.17 ± 0.04***	0.97 ± 0.06***,##
Tibialis	0.54 ± 0.02	0.42 ± 0.03***	0.41 ± 0.04**
Soleus	0.08 ± 0.01	0.07 ± 0.00*	0.07 ± 0.01*
Fat weights			
Epididymis	3.78 ± 0.19	2.73 ± 0.36*	1.79 ± 0.30***
Perirenal	2.58 ± 0.28	1.53 ± 0.45	0.64 ± 0.34**
Mesentery	1.41 ± 0.13	0.95 ± 0.29	0.40 ± 0.18**
Organ weights			
Liver	10.36 ± 0.33	7.69 ± 0.56**	6.69 ± 0.31***
Spleen	0.63 ± 0.03	0.48 ± 0.02**	0.49 ± 0.03**

Data are expressed as the mean ± SE of 5 rats; all weight data are expressed in g. TW, tumor weight; TV, tumor volume; BW, body weight; CTW, converted tumor weight. Rats were implanted subcutaneously with either 85As2 cells (1×10^6 or 1×10^7 cells/site) or saline alone in both flanks. TV was estimated using the following equation: TV (cm^3) = major axis (cm) × minor axis (cm) × minor axis (cm) × 1/2, and the TV was converted to tumor weight (mg)/mm^3. TW and TV are expressed as the total for both sites. Values for bilateral tissues represent the mean of those for the 2 unilateral tissues. BW comparisons between the control group and 85As2 groups at 4 wk after implantation showed the following relationship: %control (%) = BW of each 85As2 group/BW of control group × 100. BW comparisons between peak BW and BW at 4 wk after implantation in each 85As2 group showed the following relationship: %peak body weight (%) = BW (− TW) at 4 wk after implantation/peak BW (− CTW) × 100. Differences between groups were evaluated using Student's *t*-test. Differences in TW and TV between the control group and 85As2 groups were evaluated using the Kruskal-Wallis test, followed by a post hoc Dunn's multiple comparison test. *$P < 0.05$, **$P < 0.01$, and ***$P < 0.001$ vs. the control group; #$P < 0.05$ and ##$P < 0.01$ vs. the 85As2 cell 1×10^6 cell group; †$P < 0.05$ vs. each peak BW.

(PVN), arcuate nucleus (ARC), and lateral hypothalamic area (LHA) were identified according to the Paxinos and Watson (48) atlas and confirmed by microscopy. Hybridization was conducted under a Nescofilm coverslip (Bando Chemical, Osaka, Japan). [^{35}S]3′-end-labeled deoxyoligonucleotides complementary to transcripts coding for neuropeptide Y (*NPY*; 5′-GGA GTA GTA TCT GGC CAT GTC CTC TGC TGG CGC GTC-3′), agouti-related protein (*AgRP*; 5′-CGA CGC GGA GAA CGA GAC TCG CGG TTC TGT GGA TCT AGC ACC TCT GCC-3′), proopiomelanocortin (*POMC*; 5′-CTT CTT GCC CAG CGG CTT GCC CCA GCA GAA GTG CTC CAT GGA CTA GGA-3′), cocaine- and amphetamine-regulated transcript (*CART*; 5′-TGG GGA CTT GGC CGT ACT TCT TCT CAT AGA TCG GAA TGC-3′), orexin (5′-TTC GTA GAG ACG GCA GGA ACA CGT CTT CTG GCG ACA-3′), corticotropin-releasing hormone (*CRH*; 5′-CAG TTT CCT GTT GCT GTG AGC TTG CTG AGC TAA CTG CTC TGC CCT GGC-3′), and melanin-concentrating hormone (*MCH*; 5′-CCA ACA GGG TCG GTA GAC TCG TCC CAG CAT-3′) were used as gene-specific probes (28, 30, 31, 43, 62). Total counts of 6×10^5 counts·min^{-1}·slide^{-1} for NPY, AgPR, POMC, CART, MCH, and CRH and 4×10^5 counts·min^{-1}·slide^{-1} for orexin were used. Hybridized sections containing the ARC, LHA, and PVN regions were exposed to autoradiography film (Hyperfilm; Amersham, Buckinghamshire, UK) for 4 days for orexin and 7 days for NPY, AgRP, POMC, CART, MCH, and CRH. Autoradiographic images were captured at ×40 magnification and quantified using an MCID imaging analyzer (Imaging Research, St. Catherines, ON, Canada). The images were captured by a charge-coupled device camera (Dage-MTI, Michigan City, IN). Mean absorbance was measured and compared with simultaneously exposed ^{14}C microscale samples (Amersham). The standard curve was fitted according to the absorbance of the ^{14}C microscale on the same film.

Respiratory metabolism. Oxygen consumption was measured with an O_2/CO_2 metabolism-measuring system (MK-5000RQ; Muromachi Kikai, Tokyo, Japan) (33, 45). Each rat was kept unrestrained in a sealed chamber with an airflow of 0.5 l/min at 25°C for 20 h without food. Air was sampled every 3 min, and oxygen consumption ($\dot{V}O_2$) and carbon dioxide production ($\dot{V}CO_2$) were calculated (ml·min^{-1}·kg^{-1}). Locomotor activity was measured simultaneously with an attached device. The respiratory quotient (RQ) was calculated by dividing $\dot{V}CO_2$ by $\dot{V}O_2$. Metabolic calories (E) were calculated using the system software as follows: E (cal·min^{-1}·kg^{-1}) = (1.07 × RQ + 3.98) × $\dot{V}O_2$/body weight.

Palliative therapeutic studies using rikkunshito. Rikkunshito was manufactured by Tsumura (Tokyo, Japan) by spray-drying a hot water

Fig. 2. Effects of 85As2 cell implantation at different concentrations on body weight (*A*), tumor volume (*B*), food intake (*C*), water intake (*D*), FFM (*E*), FM (*F*), and TBW (*G*) in nude rats. Rats were inoculated sc with 85As2 cells (1×10^6 or 1×10^7 cells/each site) or saline (control) in both flanks at *week 0*. Each data point represents the mean ± SE of 5–10 rats (0–2 wk: 10 rats; 3–4 wk: 5 rats). *H*: food intake comparisons between the MKN45cl85 group and 85As2 groups ≤4 wk after implantation. Rats were inoculated sc with MKN45cl85 or 85As2 cells in both flanks (1×10^7 cells/each site) at *week 0*. Rats inoculated with saline served as a control group. Each data point represents the mean ± SE of 9–10 rats. Differences between groups were evaluated using Student's *t*-test or Welch's *t*-test. *$P < 0.05$, **$P < 0.01$, ***$P < 0.001$ vs. the control group.

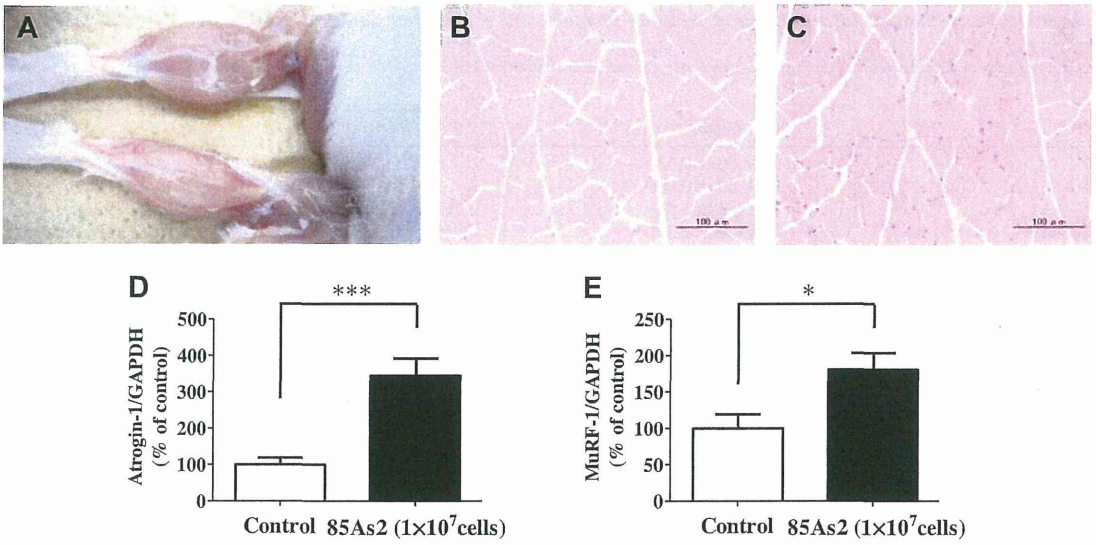

Fig. 3. Atrophy and expression of E3 ubiquitin ligases in the gastrocnemius muscle in 85As2-bearing cachectic rats 4 wk after implantation. Nude rats were inoculated subcutaneously with 85As2 cells (1×10^7 cells/each site) or saline (control) in both flanks at *week 0*. *A*: macroscopic observation of the gastrocnemius muscle in a control rat (*top* muscle in the photo) and cachectic rat (*bottom* muscle in the photo). *B* and *C*: histological observation of the gastrocnemius muscle tissue in a control rat (*B*) and cachectic rat (*C*). *D* and *E*: expression of the E3 ubiquitin ligases atrogin-1 (*D*) and muscle RING finger 1 (MuRF-1; *E*) in gastrocnemius muscle tissue. Each bar represents the mean ± SE of 7–8 rats. Differences between groups were evaluated using the Mann-Whitney *U*-test. $*P < 0.05$ and $***P < 0.001$ vs. the control group.

extract from the following eight crude drugs to form a powdered extract: *Atractylodis lanceae rhizoma* (4.0 g), *Ginseng radix* (4.0 g), *Pinelliae tuber* (4.0 g), *Hoelen* (4.0 g), *Zizyphi fructus* (2.0 g), *Aurantii nobilis pericarpium* (2.0 g), *Glycyrrhizae radix* (1.0 g), and *Zingiberis rhizoma* (0.5 g). The powdered rikkunshito extract was obtained from Tsumura. For oral administration into the stomach using a disposable sonde, rikkunshito was dissolved in distilled water (DW) at 10 g/ml in our laboratory. Rats were implanted subcutaneously (sc) with 85As2 cells in both flanks (1×10^7 cells/each site) on *day −14*. Rats inoculated with saline served as the non-tumor-bearing control group. Tumor-bearing rats were divided into two groups: a treatment (85As2 + rikkunshito) group and a tumor-bearing control (85As2 + DW) group. The treatment group was administered rikkunshito orally twice daily at 1,000 $mg \cdot kg^{-1} \cdot day^{-1}$ for 7 days (from *days 0* to *6*). The tumor-bearing control group was administered DW (10 ml/kg) over the same period. Non-tumor-bearing rats (control + DW group) were also administered DW over the same period. Tumor growth was measured weekly. Body weight and food and water intake were measured weekly until *day 0* and were measured daily thereafter. Food and water intake data after rikkunshito or DW administration are expressed as the daily, cumulative value from *days 0* to *7* or average value from *days 2* to *7*, and body weight data are expressed as body weight minus converted tumor weight. Body composition was measured on *days −14* (before tumor implantation), *0* (before administration), and *6* (after administration). Rats were anesthetized with isoflurane on *day 7*, and muscle and adipose tissues were immediately dissected and weighed.

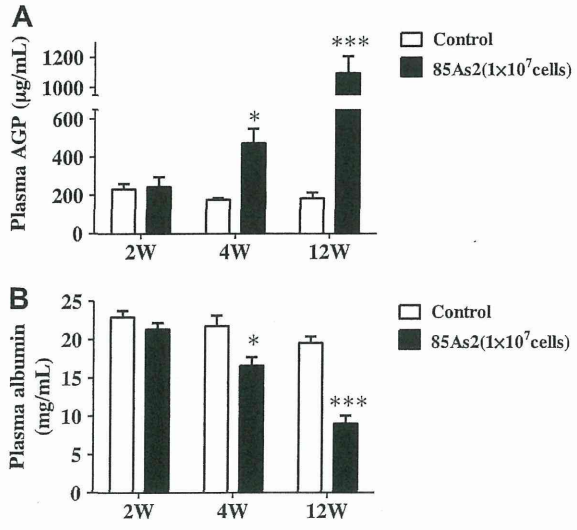

Fig. 4. Plasma levels of α1-acid glycoprotein (AGP; *A*) and albumin (*B*) at 2, 4, and 12 wk after 85As2 cell implantation in nude rats. Rats were inoculated sc with 85As2 cells (1×10^7 cells/each site) or saline (control) in both flanks at *week 0*. Each bar represents the mean ± SE of 5 rats. Differences between groups were evaluated using Student's *t*-test or Welch's *t*-test. $*P < 0.05$ and $***P < 0.001$ vs. the control group.

Statistical analyses. All data are expressed as means ± SE. Differences between groups were evaluated using the Student's *t*-test, paired *t*-test, Welch's *t*-test, Mann-Whitney *U*-test, one-way analysis of variance followed by a post hoc Dunnett's multiple comparison test, or Kruskal-Wallis test followed by a post hoc Dunn's multiple comparison test. A *P* value of <0.05 was considered significant.

RESULTS

Implantation of MKN45cl85 and 85As2 cells induced cancer cachexia in rats. Subcutaneous implantation of either MKN45cl85 or 85As2 cells in rats induced progressive tumor growth beginning 1 wk after implantation and affected body weight and composition. Body weight was markedly reduced 2 wk after implantation of MKN45cl85 and 85As2 cells compared with controls, and thereafter, the differences gradually increased (Fig. 1, *A* and *B*). Additionally, all body composition parameters (FFM, FM, and TBW) were significantly lower in the MKN45cl85 and 85As2 groups than in the control group (Fig. 1, *C–E*). Moreover, all muscle and adipose tissue weights

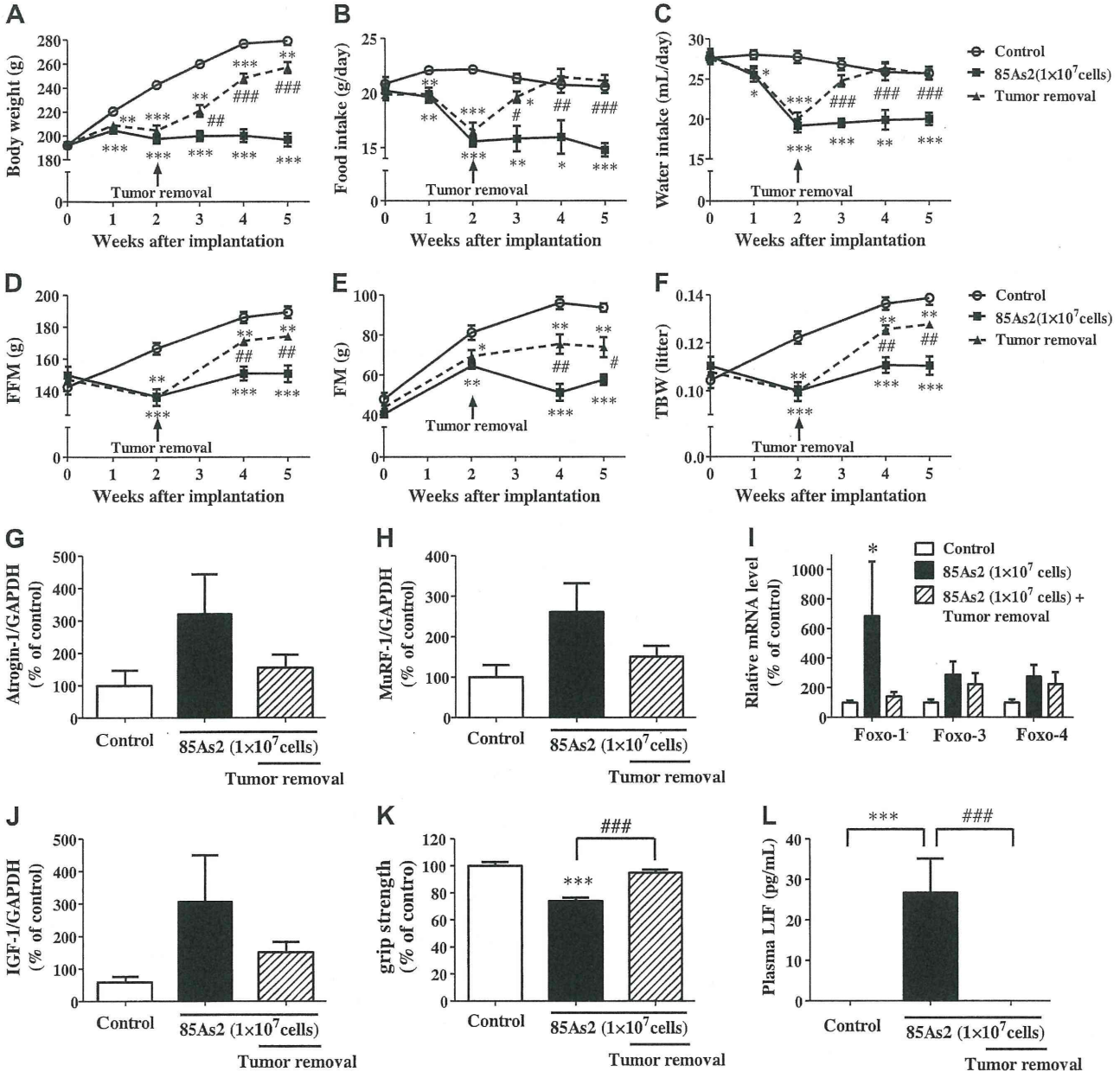

Fig. 5. Effects of tumor removal on body weight (*A*), food intake (*B*), water intake (*C*), FFM (*D*), FM (*E*), TBW (*F*), atrogin-1 (*G*), MuRF-1 (*H*), forkhead box O (*Foxo*; *I*), insulin-like growth factor-1 (*IGF-1*; *J*), grip strength (*K*), and plasma leukemia inhibitory factor (LIF; *L*) levels in nude rats implanted with 85As2 cells (1×10^7 cells/each site) or saline (control) in both flanks at *week 0*. Plasma and the gastrocnemius muscle of the rats were collected 5 wk after implantation. Each data point or bar represents the mean ± SE of 8–9 rats (*A–C*, *K*, and *L*). Each data point or bar represents the mean ± SE of 5 rats (*D–J*). Differences between groups were evaluated using Student's *t*-test or the Mann-Whitney *U*-test. Differences in plasma LIF levels between groups were evaluated using the Kruskal-Wallis test, followed by post hoc Dunn's multiple comparison test. $^*P < 0.05$, $^{**}P < 0.01$, and $^{***}P < 0.001$ vs. the control group; $\#P < 0.05$, $\#\#P < 0.01$, and $\#\#\#P < 0.001$ vs. the corresponding 85As2 group.

were significantly reduced in cachectic rats at 12 wk after implantation compared with control rats (Fig. 1*F*). Symptoms of cancer cachexia, including weight loss, low FM and FFM, and wasting of muscle and adipose tissues, were more pronounced in the 85As2 group than in the MKN45cl85 group.

85As2-induced cancer cachexia rat model characterization. Because the 85As2 model induced more severe cancer cachexia in rats than the MKN45cl85 model, the 85As2-induced cancer cachexia model was characterized further. Tumor volume grew progressively in a cell concentration-dependent manner, reaching 1.94 ± 0.57 and 4.38 ± 0.68 cm^3 at 4 wk after implantation of 1×10^6 and 1×10^7 85As2 cells, respectively (Fig. 2*B*). The body weight of the control group continued to increase during the experiment, whereas the body weight of the 85As2 groups did not. Body weight loss was higher in the 85As2 groups than in the control group beginning

Table 2. *Plasma levels of human cytokines in the cancer cachexia rat models and cell culture supernatants*

Time after Inoculation	Cells	IL-1β	IL-6	IL-8	TNFα	LIF
Plasma (2 wk)						
Control		<2.44	<2.44	<2.44	<2.44	<2.44
85As2	1×10^6	<2.44	<2.44	<2.44	<2.44	5.35 ± 3.49
MKN45cl85	1×10^7	<2.44	<2.44	<2.44	<2.44	12.94 ± 2.02*
Plasma (4 wk)						
Control		<2.44	<2.44	<2.44	<2.44	<2.44
85As2	1×10^6	<2.44	<2.44	<2.44	<2.44	24.38 ± 5.99
MKN45cl85	1×10^7	<2.44	<2.44	<2.44	<2.44	41.77 ± 11.08*
Plasma (12 wk)						
Control		<2.44	<2.44	<2.44	<2.44	<2.44
85As2	1×10^7	<2.44	<2.44	39.88 ± 25.14**	<2.44	321.18 ± 42.02**
MKN45cl85	1×10^7	<2.44	<2.44	<2.44	<2.44	75.78 ± 17.51
Supernatant (24 h)						
85As2	5×10^5	ND	ND	10.36 ± 0.70***	ND	611.74 ± 3.84**
MKN45cl85	5×10^5	ND	ND	321.47 ± 22.98	ND	416.00 ± 26.71
Supernatant (48 h)						
85As2	5×10^5	ND	ND	19.02 ± 3.93***	ND	937.29 ± 18.48**
MKN45cl85	5×10^5	ND	ND	559.98 ± 25.16	ND	724.91 ± 22.50

Cytokine levels in cell culture supernatants are expressed as the mean ± SE of triplicate wells in pg/ml, and plasma cytokine levels are expressed as the mean ± SE (pg/ml) values for 4–5 rats. LIF, leukemia inhibitory factor; ND, not detectable (below the minimum detection limit of the assay). Rats were implanted subcutaneously with MKN45cl85 or 85As2 cells (1×10^6 or 10^7 cells/site) or saline alone in both flanks. Differences in plasma cytokine levels between groups were evaluated using the Kruskal-Wallis test, followed by a post hoc Dunn's multiple comparison test (*$P < 0.05$ and **$P < 0.01$ vs. the corresponding control group). Supernatants were collected from 24- or 48-h incubation cultures. Differences in the cytokine levels in cell culture supernatants for the groups were evaluated using Student's *t*-test (**$P < 0.01$ and ***$P < 0.001$ vs. the corresponding MKN45cl85 group).

at 2 wk after implantation and became significant at 3 and 2 wk after implantation of 1×10^6 and 1×10^7 cells, respectively (Fig. 2*A*). The differences in body weight between the 85As2-implanted groups and corresponding control groups were greatest at 4 wk after implantation. The differences in body weight between the 85As2 groups and control group were 70.1–74.3 and 82.7–84.7% regardless of body weight with or without the tumor weight at 4 wk after implantation of 1×10^7

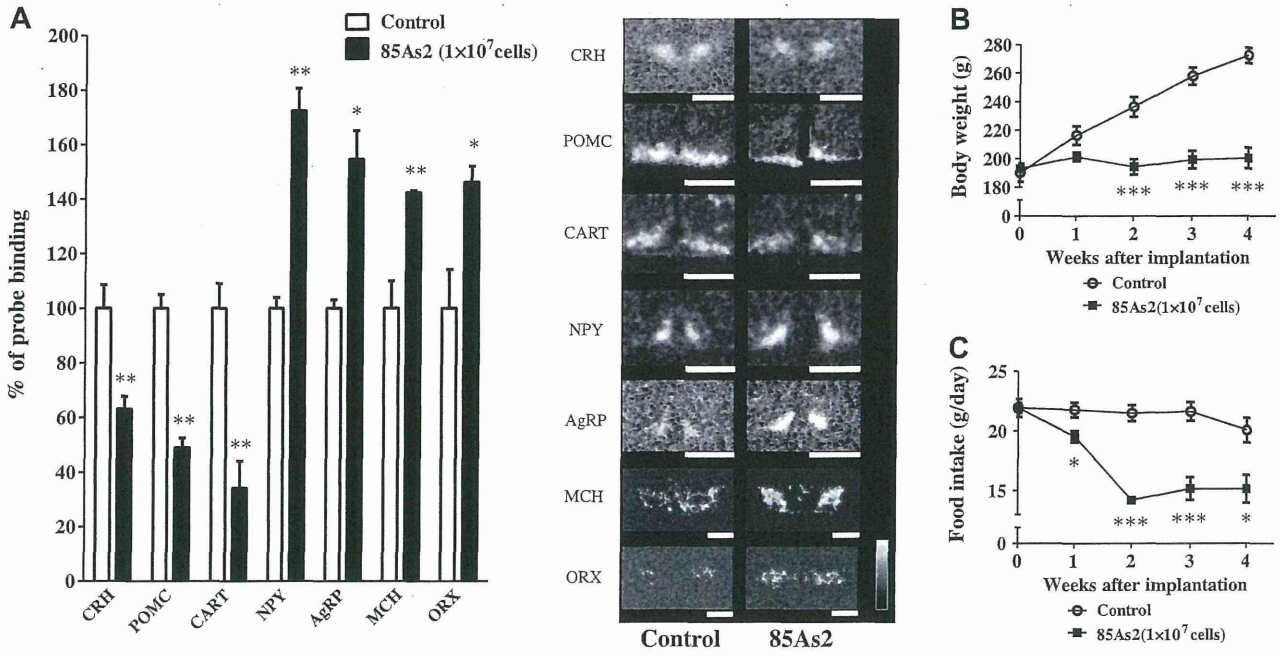

Fig. 6. *A*: mRNA expression of neuropeptide Y (*NPY*), agouti-related protein (*AgRP*), proopiomelanocortin (*POMC*), and cocaine- and amphetamine-regulated transcript (*CART*) in the arcuate nucleus (ARC), corticotropin-releasing hormone (*CRH*) in the paraventricular nucleus (PVN), and orexin (*ORX*) and melanin-concentrating hormone (*MCH*) in the lateral hypothalamic area (LHA) in control and 85As2-induced cachectic rats 4 wk after implantation. Nude rats were inoculated subcutaneously with 85As2 cells (1×10^7 cells/each site) or saline (control) in both flanks at *week 0*. In situ hybridization was measured 4 wk after implantation. Representative autoradiographs of sections hybridized by a ^{35}S-labeled oligodeoxynucleotide probe complementary to mRNA for all the peptides mentioned in *A*. Signal intensity ranges from high (black bars) to low (open bars). Black bar = 1 mm. *B* and *C*: time course changes in body weight (*B*) and food intake (*C*). Changes in body weight and food intake were evident at 4 wk after implantation. Each bar or data point represents the mean ± SE of 6 rats. Differences between groups were evaluated using Student's *t*-test. *$P < 0.05$, **$P < 0.01$, and ***$P < 0.001$vs. the control group.

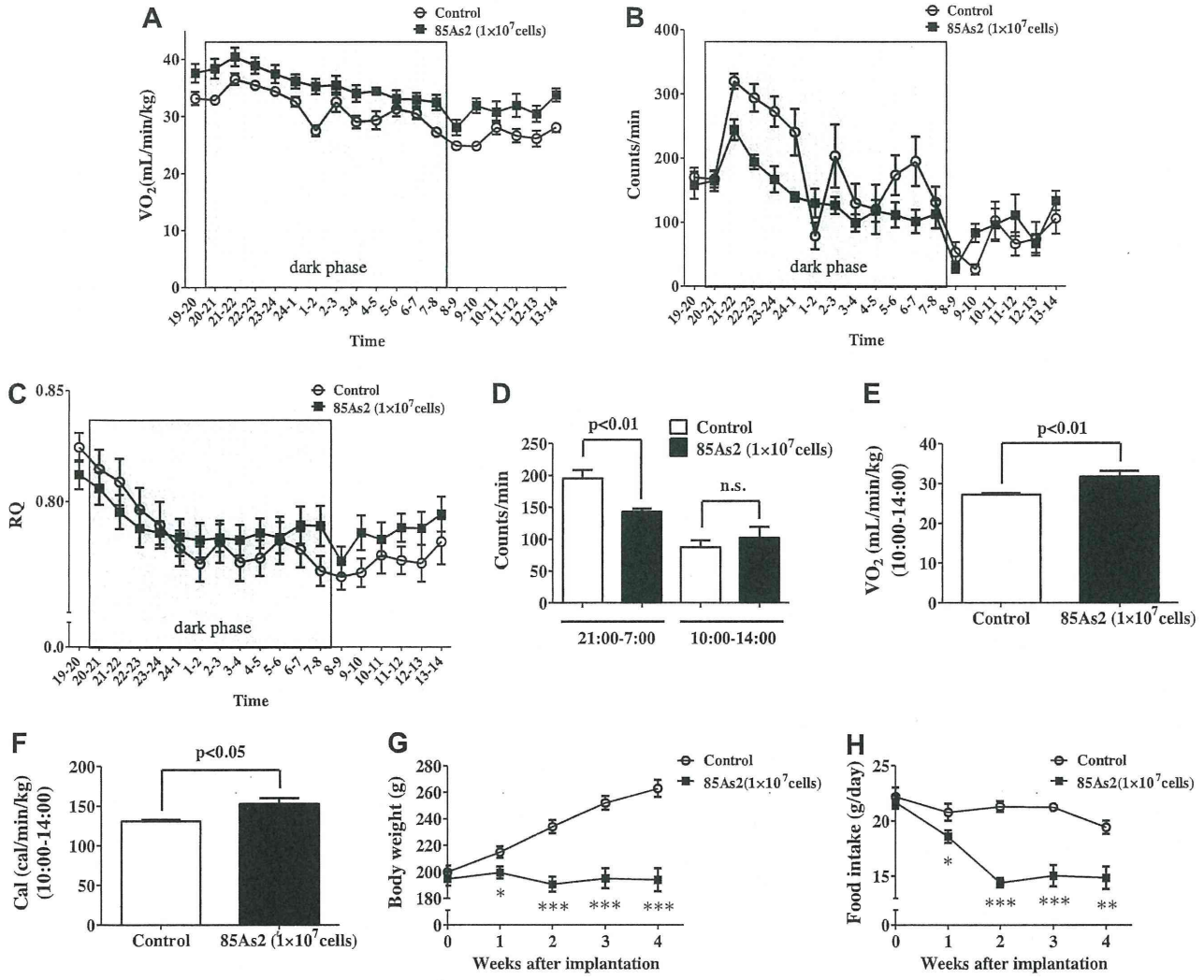

Fig. 7. Time course changes in oxygen consumption ($\dot{V}O_2$, ml·min^{-1}·kg^{-1}; *A*), locomotor activity (*B*), respiratory quotient (RQ; *C*), average cumulative locomotor activity (*D*), $\dot{V}O_2$ (ml·min^{-1}·kg^{-1}) (*E*), and metabolic calories (cal·min^{-1}·kg^{-1}; *F*) from 1000 to 1400 at 4 wk after 85As2 cell implantation in nude rats. Rats were inoculated sc with 85As2 cells (1×10^7 cells/each site) or saline (control) in both flanks at *week 0*. Respiratory metabolism was measured 4 wk after implantation. Changes in body weight (*G*) and food intake (*H*) over time. Changes in body weight and food intake were evident at 4 wk after implantation. Each data point or bar represents the mean ± SE of 7 rats. Differences between groups were evaluated using Student's *t*-test or the Mann-Whitney *U*-test. $*P < 0.05$, $**P < 0.01$, and $***P < 0.001$ vs. the control group.

and 1×10^6 cells, respectively (Table 1). Comparison between peak body weight and body weight 4 wk after implantation showed body weight loss in each cachectic rat (1×10^7 cells, 88.0 ± 3.5%; and 1×10^6 cells, 94.4 ± 2.7%). These comparisons were made using the corresponding individual peak body weight. All body composition parameters (FFM, FM, and TBW) were also substantially lower in the 85As2 groups than in the control groups (Fig. 2, *E–G*).

Reductions in food and water intake were observed beginning at 1 wk after implantation in the 85As2 groups compared with the corresponding control groups and became significant 2–4 wk later (food intake: 1×10^7 cells, 73.5–78.7%; and 1×10^6 cells, 89.0–90.7%; water intake: 1×10^7 cells, 71.2–80.1%; and 1×10^6 cells, 83.4–88.7%; Fig. 2, *C* and *D*). Similarly to the 85As2-induced cachexia model, MKN45cl85-implanted rats also exhibited marked decreases in food intake (Fig. 2*H*). However, the decrease in food intake was less pronounced in MKN45cl85-implanted rats than in 85As2-implanted rats (MKN45cl85, 1×10^7 cells, 83.8–87.0% compared with the corresponding control groups).

Muscle (greater pectoral, gastrocnemius, tibialis, and soleus), adipose tissue (epididymal, perirenal, and mesentery fat), liver, and spleen weights decreased substantially in a cell concentration-dependent manner at 4 wk after implantation in cachectic rats compared with that in control rats (Table 1). Macroscopic and histological observations confirmed gastrocnemius muscle atrophy in the 85As2 group (1×10^7 cells) at 4 wk after implantation (Fig. 3, *A–C*). Furthermore, all cells in Fig. 3, *B* and *C* (control, $n = 51$; 85As2, $n = 75$), were measured, and the cross-sectional area, perimeter, Feret diameter, and minimum Feret diameter were calculated. The cross-sectional area (1,460.4 ± 76.3 vs. 2,023.9 ± 85.2 μm^2, $P <$

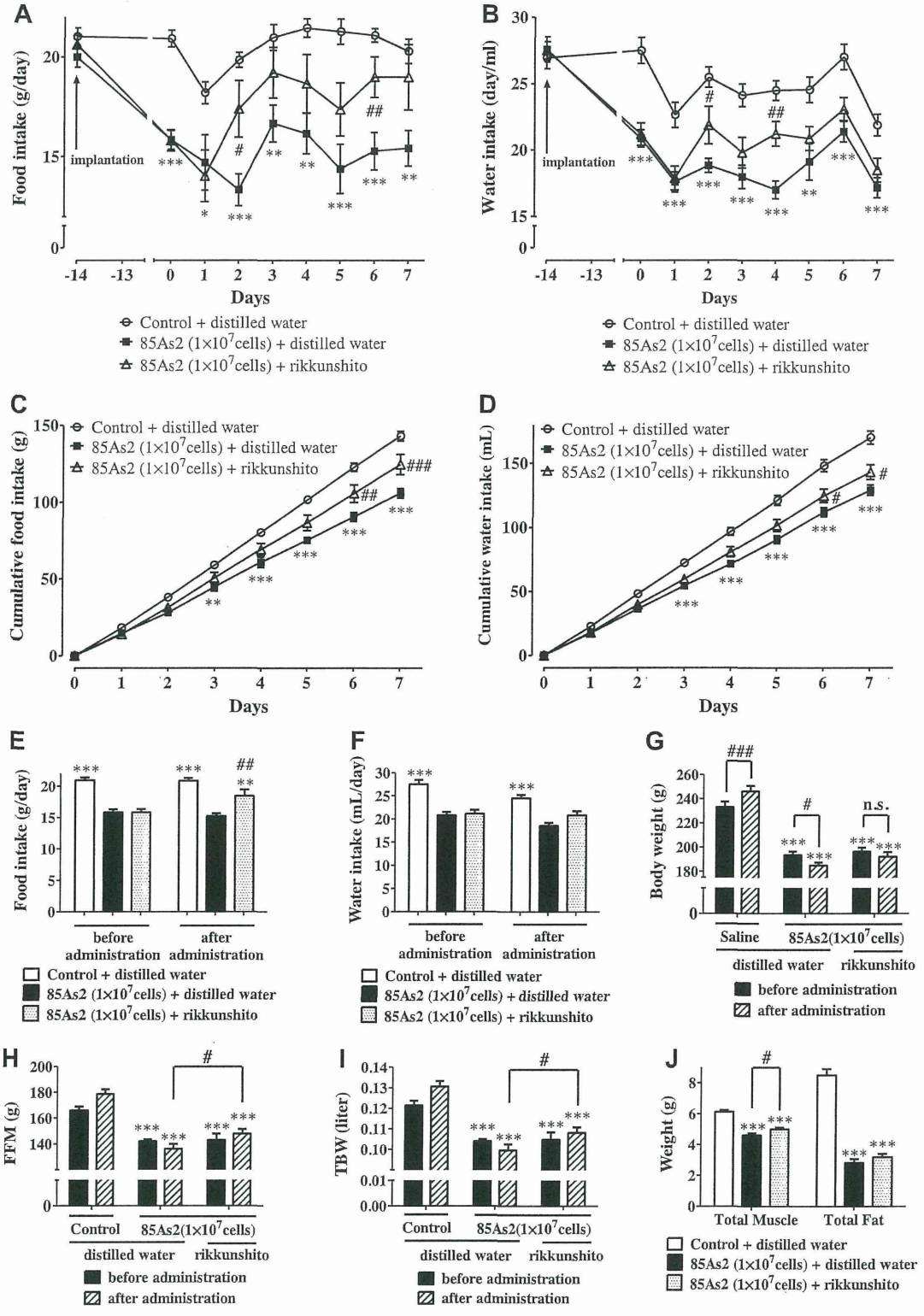
A
Food intake (g/day)
implantation
Days
Control + distilled water
85As2 (1×10^7cells) + distilled water
85As2 (1×10^7cells) + rikkunshito
B
Water intake (day/ml)
implantation
Days
Control + distilled water
85As2 (1×10^7cells) + distilled water
85As2 (1×10^7cells) + rikkunshito
C
Cumulative food intake (g)
Days
Control + distilled water
85As2 (1×10^7cells) + distilled water
85As2 (1×10^7cells) + rikkunshito
D
Cumulative water intake (mL)
Days
Control + distilled water
85As2 (1×10^7cells) + distilled water
85As2 (1×10^7cells) + rikkunshito
E
Food intake (g/day)
before administration
after administration
Control + distilled water
85As2 (1×10^7cells) + distilled water
85As2 (1×10^7cells) + rikkunshito
F
Water intake (mL/day)
before administration
after administration
Control + distilled water
85As2 (1×10^7cells) + distilled water
85As2 (1×10^7cells) + rikkunshito
G
Body weight (g)
n.s.
Saline
85As2(1×10^7cells)
distilled water
rikkunshito
before administration
after administration
H
FFM (g)
Control
85As2(1×10^7cells)
distilled water
rikkunshito
before administration
after administration
I
TBW (liter)
Control
85As2(1×10^7cells)
distilled water
rikkunshito
before administration
after administration
J
Weight (g)
Total Muscle
Total Fat
Control + distilled water
85As2 (1×10^7cells) + distilled water
85As2 (1×10^7cells) + rikkunshito

0.0001), perimeter (151.1 ± 4.3 vs. 179.2 ± 4.1 μm, $P <$ 0.0001), Feret diameter (57.5 ± 1.7 vs. 67.2 ± 1.8 μm, $P <$ 0.001), and minimum Feret diameter (36.4 ± 1.1 vs. 44.1 ± 1.2 μm, $P < 0.0001$) were lower in the 85As2 group than in the control group. A corresponding increase in the expression of muscle-specific E3 ubiquitin ligases (atrogin-1 and MuRF-1; Fig. 3, *D–E*) and reduction in grip strength were also observed (Fig. 5*K*). Three Foxo family members present in skeletal muscle (*Foxo1*, *Foxo3*, and *Foxo4*) (49) were upregulated in the gastrocnemius muscles of the 85As2-induced cachectic rats, and the increase in *Foxo1* was particularly prominent (Fig. 5, *G–I*). *IGF-1* was upregulated in cachectic rats (nonsignificant) (Fig. 5*J*). Plasma albumin level decreased in 85As2 (1×10^7 cells)-bearing cachectic rats, whereas the level of α1-acid glycoprotein, the murine counterpart of human C-reactive protein, was increased (Fig. 4, *A* and *B*). Importantly, tumor removal restored body weight loss, food and water intake, body composition (FFM, FM, and TBW), and grip strength (Fig. 5, *A–F* and *K*). Furthermore, tumor removal reduced the increased expression levels of not only atrogin-1 (85As2, 321.2% ± 123.2%; tumor removal, 155.2% ± 40.8%) and *MuRF-1* (85As2, 261.5% ± 71.3%; tumor removal, 150.7% ± 27.0%) but also *Foxo-1* (85As2, 683.7% ± 368.7%; tumor removal, 140.5% ± 29.6%) in the gastrocnemius muscle (Fig. 5, *G–I*).

Cytokine levels. To investigate the underlying causes of cancer cachexia, the plasma concentrations of several proinflammatory cytokines were measured. Human LIF levels were remarkably elevated in a cell concentration- and time-dependent manner in rats implanted with 85As2 cells, whereas the levels of human IL-1β, IL-6, and TNFα were not elevated in this model at 12 wk (Table 2). Similar results were obtained in MKN45cl85-implanted rats at 12 wk. Additionally, rat IL-1β, IL-6, KC, and TNFα levels were below detection limits, and IFNγ levels were unchanged in both rat models (data not shown). Moreover, human LIF production was observed in cell culture supernatants from both cell lines, although 85As2 cells produced substantially higher amounts of LIF than MKN45cl85 cells (Table 2). Human IL-8 production was also observed in both cell lines. Furthermore, tumor removal reversed the increase in plasma LIF levels in 85As2-bearing cachectic rats (Fig. 5*L*).

Gene expression of hypothalamic orexigenic/anorexigenic peptides in the 85As2-induced cachexia model. Cachexia symptoms such as body weight loss and anorexia were induced in rats implanted with 85As2 cells (1×10^7 cells; Fig. 6, *B* and *C*). Hypothalamic feeding-regulating peptide levels were evaluated 4 wk after implantation of 85As2 cells. Orexigenic peptide mRNA levels (*NPY* and *AgRP* in the ARC, *ORX* and *MCH* in the LHA) were higher in 85As2 cachectic rats than in control rats, whereas anorexigenic peptide mRNA levels (*POMC* and *CART* in the ARC, *CRH* in the PVN) were lower in cachectic rats than in control rats (Fig. 6*A*).

Respiratory metabolism in the 85As2-induced cachexia model. Cachexia symptoms such as body weight loss and anorexia were induced in rats implanted with 85As2 cells (1×10^7 cells; Fig. 7, *G* and *H*). $\dot{V}O_2$ was higher in 85As2-induced cachectic rats than in control rats 4 wk after implantation (Fig. 7*A*). Locomotor activity was noticeably lower during the "active" overnight period in cachectic rats than in control rats (Fig. 7, *B* and *D*). RQ, $\dot{V}O_2$, and metabolic calorie levels were significantly higher in cachectic rats than in control rats during the daytime period, although locomotor activity was not different between the groups during this time period (Fig. 7, *C–F*).

Rikkunshito ameliorates cachexia in the 85As2-induced cachexia model. Rikkunshito increased food and water intake rates (Fig. 8, *A–F*) and alleviated body weight loss, FFM, TBW, and total musculature weight loss in 85As2-induced cachectic rats (Fig. 8, *G–J*).

DISCUSSION

Herein, we established novel stomach cancer cachexia models by implanting nude rats with MKN45cl85 and 85As2 cells, both of which were derived from the human stomach cancer cell line MKN-45. These models enabled us to sequentially evaluate anorexia and body composition changes (low FFM) that correspond to poor QOL in human cancer patients. In addition to anorexia and low FFM, the cachexia models showed significant weight loss, reduced musculature and muscle strength, and abnormal biochemistry (increased inflammatory marker levels and low serum albumin levels), thereby fulfilling the cachexia diagnostic criteria (20). Interestingly, cancer cachexia developed earlier and was more severe in the 85As2-bearing model than in the MKN45cl85-bearing model, indicating that 85As2 cells derived from peritoneal dissemination possessed an enhanced ability to cause cachexia. Indeed, the presence of peritoneal metastasis promotes cachexia and is associated with a poor prognosis and low QOL in patients with advanced-stage stomach cancer. Our 85As2-bearing model may provide a useful tool for further study into the mechanisms and potential treatment of cancer cachexia.

Characterization of the 85As2-induced cachexia rat model showed marked weight loss and reductions in food and water

Fig. 8. Effects of rikkunshito on anorexia and body composition changes in the 85As2-induced cancer cachexia model. Changes in food intake (*A*), water intake (*B*), cumulative food intake (*C*), and cumulative water intake (*D*) over time. Comparison of food intake (*E*), water intake (*F*), body weight (*G*), FFM (*H*), TBW (*I*), and total muscle and fat weight (*J*) before and after rikkunshito administration. Rats were implanted sc with 85As2 cells in both flanks (1×10^7 cells/each site) on *day −14*. Rikkunshito ($1\ g \cdot kg^{-1} \cdot day^{-1}$) or distilled water was administered orally twice a day for 7 days from *day 0*. Rats inoculated with saline served as a control group and were similarly administered distilled water. Each data point or bar represents the mean ± SE of 10–11 rats. Differences between saline-implanted and 85As2-implanted rats were evaluated using Student's *t*-test; $*P < 0.05$, $**P < 0.01$, and $***P < 0.001$ vs. the corresponding control + distilled water-treated group (*A*, *B*, and *G–J*). Differences between rikkunshito and distilled water treatments were evaluated using Student's *t*-test; $\#P < 0.05$ and $\#\#P < 0.01$ vs. the corresponding 85As2 + distilled water-treated group (*A*, *B*, and *H–J*). Differences between groups in the time course of cumulative food and water intake were evaluated using 2-way repeated-measures ANOVA, followed by post hoc Bonferroni test; $**P < 0.01$ and $***P < 0.001$ vs. the corresponding control + distilled water-treated group; $\#P < 0.05$, $\#\#P < 0.01$, and $\#\#\#P < 0.001$ vs. the corresponding 85As2 + distilled water-treated group (*C* and *D*). Differences between groups were evaluated using a 1-way ANOVA, followed by post hoc Dunnett's multiple comparison test; $**P < 0.01$ and $***P < 0.001$ vs. the 85As2 + distilled water-treated group (*E* and *F*). Differences before and after administration of either rikkunshito or distilled water were evaluated using the paired *t*-test; $\#P < 0.05$, $\#\#P < 0.01$, $\#\#\#P < 0.001$ vs. the corresponding before-administration group (*E* and *G*).

intake. Furthermore, 85As2-induced cachexia decreased FFM, FM, and TBW, which was confirmed by histological observations. In the present experimental models, tumor growth or cachexia developed very early. However, young rats (aged 8 wk at the time of implantation) were used; therefore, senescence, which is common in human cancer, may have been a limitation of the study. Although 85As2 cell implantation can cause peritoneal dissemination accompanied by ascites (63), the decreased food intake in our model was not associated with either condition. Reduced FFM in cachectic rats was thought to be caused primarily by wasting skeletal muscle and organ tissues, as evidenced by the reduction in all measured musculature weights, muscle atrophy (e.g., gastrocnemius muscle), and reduced spleen and liver weights. Because intracellular skeletal muscle proteins are degraded primarily by the ubiquitin-proteasome system (2, 16), increased expression of the E3 ubiquitin ligases atrogin-1 and *MuRF-1* likely contributed to skeletal muscle loss by accelerating muscle protein breakdown during cancer cachexia development, as these enzymes have been associated with muscle wasting in other cancer cachexia animal models (2, 16). Moreover, increased expression of atrogin-1 and *MuRF-1* in the gastrocnemius muscles of cachectic rats has been associated with increased expression of *Foxo*, the master regulators of muscle-specific E3 ligases, and increased *Foxo* expression has been shown in cancer cachexia models (49). In our study, *Foxo1*, *Foxo3*, and *Foxo-4* were upregulated in 85As2-induced cachectic rats, and their increased expression was thought to be associated with the increased expression of atrogin-1 and *MuRF-1*. Notably, the elevation of Foxo1 levels was prominent, and its blockade suppressed cachectic muscle atrophy (36). Expression of the protein synthetic factor IGF-I has been reported to decrease in cancer cachexia models (16). However, *IGF-1* expression did not decrease in cachectic rats; rather, it unexpectedly increased, although the increase was not significant. Taken together, our findings indicated that protein degradation pathways in skeletal muscle were activated in 85As2-induced cachectic rats. Importantly, tumor removal reversed the cachexia symptoms, including body weight loss, decreased food and water intake, body composition changes, and increased expression of genes that accelerate muscle protein breakdown such as atrogin-1, *MuRF-1*, and *Foxo-1* in 85As2-bearing cachectic rats. These findings strongly indicated that the 85As2 cancer cell xenograft induced cachexia symptoms.

Increasing evidence suggests that proinflammatory cytokines, including TNFα, IL-1, IL-6, IL-10, and TGFβ, may be involved in the development of cancer cachexia (13, 19, 58). For example, high IL-6 levels have been associated with increased inflammation (20) and weight loss in patients with non-small-cell lung, pancreatic, and prostate cancers (19, 46, 51). However, other studies have suggested that cancer cachexia is not fully attributable to IL-6 levels (53). In the present study, human and rat IL-6 were not detected in the plasma of MKN45cl85- or 85As2-tumor-bearing cachectic rats or in cell culture supernatants, making it unlikely that IL-6 was a causative factor for cancer cachexia in our experimental model. Moreover, human and rat IL-1β and TNFα were not detected in the plasma of tumor-bearing cachectic rats, and human IL-10 and TGFβ were not detected in the cell culture supernatants, which was similar to our previous results in a stomach cancer cachexia mouse model (63). In contrast, plasma levels of human LIF, a pleiotropic cytokine belonging to the IL-6 family, were markedly elevated in a cell concentration- and time-dependent manner in rats implanted with 85As2 cells. These findings are in agreement with a previous study showing higher LIF levels in a melanoma SEKI-induced cancer cachexia mouse model (39, 40). Furthermore, we found that tumor removal not only abolished the cachexia symptoms induced by 85As2 cells but also decreased plasma LIF levels to below detectable levels. Therefore, our findings strongly suggested that LIF is a cachectic factor in the 85As2-bearing cachexia model. To date, genetic polymorphisms of cytokines such as IL-1β, IL-8, and IL-10 have been implicated in cachexia pathogenesis in stomach cancer patients (5, 26, 54). Our study is the first to associate LIF with stomach cancer cachexia. Although clinical evaluation of LIF is currently ongoing, LIF may be a biomarker of pathogenesis and a therapeutic target for peritoneal dissemination and cachexia in stomach cancer.

LIF and its receptor LIF-R, a heterodimeric receptor complex consisting of the ligand-specific LIF-R and signal-transducing gp130 subunit (3), are expressed in POMC neurons in the ARC and have been shown to impact signaling in the hypothalamus. LIF has been shown to inhibit food intake by directly activating POMC neurons in the ARC and stimulating the release of α-melanocyte-stimulating hormone, which in turn transduces anorexigenic signals (27). Importantly, the blood-brain barrier is relatively permissive in the ARC, allowing the neurons to access circulating macromolecules. In fact, Pan et al. (47) showed that peripherally administered LIF reached the brain and spinal cord by crossing the blood-brain barrier. Taken together, these findings suggested that LIF produced by 85As2 and MKN45cl85 cell implantation induced cachexia symptoms, including anorexia, in the present study by affecting LIF receptor signaling pathways in POMC neurons in the ARC. Moreover, LIF may contribute to differences in the onset and severity of cachexia in the 85As2 and MKN45c185 cachexia models. However, further study is necessary to determine the contribution of other cachectic factors to the varying degrees of cancer cachexia in these models.

In the present study, hypothalamic levels of orexigenic peptide mRNAs (*NPY* and *AgRP* in the ARC, *ORX* and *MCH* in the LHA) were increased in the 85As2-induced cachexia model, whereas the levels of anorexigenic peptide mRNAs (*POMC* and *CART* in the ARC, *CRH* in the PVN) were decreased. Previous studies have shown that hypothalamic NPY release is reduced and that the feeding response to hypothalamic injection of NPY is attenuated in anorectic tumor-bearing rats despite increased hypothalamic *NPY* mRNA expression (9–12, 38). Moreover, proinflammatory signals (e.g., IL-1β) have been shown to decrease AgRP secretion but increase *AgRP* gene transcription (50). Thus, despite increases in hypothalamic *NPY* and *AgRP* mRNA expression, the anorexia induced in our model may involve impairment of NPY and AgRP release or feeding response to NPY. Interestingly, our previous study using a cisplatin-induced cachexia rat model yielded contrasting results to those of the 85As2 model, although both models exhibited decreased food intake. In the cisplatin-induced cachexia model, hypothalamic orexigenic peptide mRNA levels decreased and anorexigenic peptide mRNA levels increased (65). Cisplatin has been shown to reduce the secretion of ghrelin that activates NPY neurons,